

Tuning the HOMO–LUMO Gap of Pyrene Effectively via Donor–Acceptor Substitution: Positions 4,5 Versus 9,10

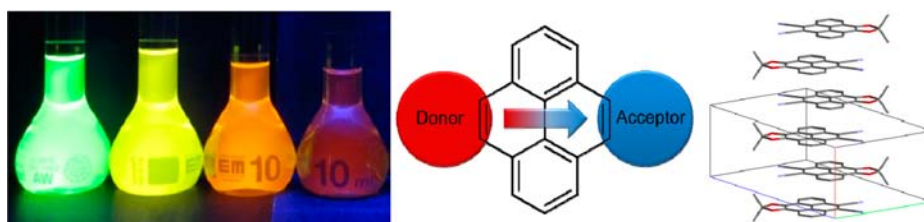
Lukas Zöphel, Volker Enkelmann, and Klaus Müllen*

Max Planck Institut for Polymer Research Ackermannweg 10, 55128 Mainz, Germany

muellen@mpip-mainz.mpg.de

Received December 19, 2012

ABSTRACT



Donor and acceptor substituents were introduced at pyrene's K-regions in order to engineer its optoelectronic properties. A study of the influence of the substitution pattern on the frontier orbitals as well as on the molecular packing is provided. A comparison with the pure donor and acceptor substituted pyrene derivatives highlights the strong impact of the presented donor–acceptor substitution.

Energy gap engineering is a crucial issue for the design of organic light-emitting, light-absorbing and semiconducting materials.¹ The use of donor and acceptor motifs is firmly established, as donor–acceptor (D–A) substitution strongly affects the levels of the frontier orbitals and thus helps to tune the optical and electronic properties of a material. Such push–pull systems with strong donor and acceptor units are known to exhibit narrowed energy gaps and strong dipoles due to the intramolecular charge transfer. Therefore, such materials have been of interest as long-wavelength absorbing dyes,² in nonlinear optics³ and as optical sensors for pH-value and solvent polarity.⁴

This concept of D–A substitution has also been applied on highly fluorescent polycyclic aromatic hydrocarbons

(PAHs) for their use in organic light-emitting diodes (OLEDs).⁵ Among these, pyrene is a well-studied and fascinating molecule due to its outstanding optical properties. Pyrene strongly emits blue light and has been frequently used as fluorescence probe⁶ and emitter material in OLEDs.⁷ Typically the easily accessible positions 1, 3, 6, and 8 are utilized to adjust the emission properties via ethynylation or arylation giving star-shaped pyrene derivatives.⁸ So far, the concept of D–A substitution has not been pursued on pyrene, most likely due to missing

(1) (a) Beaujuge, P. M.; Amb, C. M.; Reynolds, J. R. *Acc. Chem. Res.* **2010**, *43*, 1396–1407. (b) Zhang, Z. G.; Wang, J. Z. *J. Mater. Chem.* **2012**, *22*, 4178–4187. (c) Hagberg, D. P.; Marinado, T.; Karlsson, K. M.; Nonomura, K.; Qin, P.; Boschloo, G.; Brinck, T.; Hagfeldt, A.; Sun, L. *J. Org. Chem.* **2007**, *72*, 9550–9556. (d) van Müllekom, H. A. M.; Vekemans, J. A. J. M.; Havinga, E. E.; Meijer, E. W. *Mater. Sci. Eng. R-Rep.* **2001**, *32*, 1–40. (e) Li, C.; Liu, M. Y.; Pschirer, N. G.; Baumgarten, M.; Müllen, K. *Chem. Rev.* **2010**, *110*, 6817–6855.

(2) (a) Li, C.; Wonneberger, H. *Adv. Mater.* **2012**, *24*, 613–36. (b) Achelle, S.; Barsella, A.; Baudequin, C.; Caro, B.; Guen, F. R. L. *J. Org. Chem.* **2012**, *77*, 4087–4096.

(3) Kivala, M.; Diederich, F. *Acc. Chem. Res.* **2009**, *42*, 235–248.

(4) (a) Maus, M.; Rurack, K. *New J. Chem.* **2000**, *24*, 677–686. (b) Sumalekshmy, S.; Gopidas, K. R. *J. Phys. Chem. B* **2004**, *108*, 3705–3712. (c) Sumalekshmy, S.; Gopidas, K. R. *New J. Chem.* **2005**, *29*, 325–331.

(5) (a) Finlayson, C. E.; Kim, J.-S.; Liddell, M. J.; Friend, R. H.; Jung, S.-H.; Grimsdale, A. C.; Müllen, K. *J. Chem. Phys.* **2008**, *128*, 044703–10. (b) Thirion, D.; Rault-Berthelot, J. I.; Vignau, L.; Poriol, C. *Org. Lett.* **2011**, *13*, 4418–4421. (c) Chen, C.-H.; Huang, W.-S.; Lai, M.-Y.; Tsao, W.-C.; Lin, J. T.; Wu, Y.-H.; Ke, T.-H.; Chen, L.-Y.; Wu, C.-C. *Adv. Funct. Mater.* **2009**, *19*, 2661–2670. (d) Fisher, A. L.; Linton, K. E.; Kamtekar, K. T.; Pearson, C.; Bryce, M. R.; Petty, M. C. *Chem. Mater.* **2011**, *23*, 1640–1642.

(6) (a) Duhamel, J. *Acc. Chem. Res.* **2006**, *39*, 953–960. (b) Mathew, A. K.; Siu, H.; Duhamel, J. *Macromolecules* **1999**, *32*, 7100–7108. (c) Jackson, G. S.; Staniforth, R. A.; Halsall, D. J.; Atkinson, T.; Holbrook, J. J.; Clarke, A. R.; Burston, S. G. *Biochemistry* **1993**, *32*, 2554–2563. (d) Jung, K.; Jung, H.; Wu, J. H.; Prive, G. G.; Kaback, H. R. *Biochemistry* **1993**, *32*, 12273–12278.

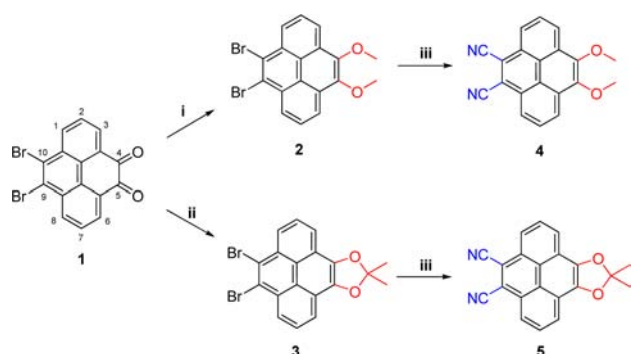
(7) Figueira-Duarte, T. M.; Müllen, K. *Chem. Rev.* **2011**, *111*, 7260–314.

(8) (a) Moorthy, J. N.; Natarajan, P.; Venkatakrishnan, P.; Huang, D. F.; Chow, T. *J. Org. Lett.* **2007**, *9*, 5215–5218. (b) Oh, J. W.; Lee, Y. O.; Kim, T. H.; Ko, K. C.; Lee, J. Y.; Kim, H.; Kim, J. S. *Angew. Chem., Int. Ed.* **2009**, *48*, 2522–2524. (c) Oh, H.; Lee, C.; Lee, S. *Org. Electron.* **2009**, *10*, 163–169.

synthetic protocols as asymmetric functionalization of PAHs has always been a challenge for organic chemists. Recently, we reported a convenient protocol for the synthesis of the asymmetric building block **1** in two steps from pyrene.⁹ **1** allows the independent conversion of the two K-regions (4,5 and 9,10) and thus provides the basis for straightforward D–A substitution. This further enables the introduction of twice as many donor and acceptor functions providing stronger electronic effects.

In this letter, we present pyrenes with D–A substituents in the K-region together with a detailed investigation of their optoelectronic properties and solid state packing. The pure donor and acceptor pyrenes have also been synthesized to compare substitution effects.

Scheme 1. Synthesis of D–A Pyrenes **4** and **5**^a



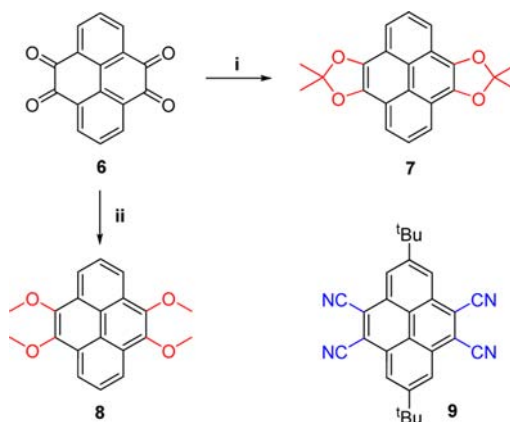
^a Conditions: *i* Na₂S₂O₄, Me₂SO₄, KOH, Bu₄NBr, H₂O/THF, 40 °C, overnight, 65%; *ii* 2-nitropropane, Na₂CO₃, acetonitrile/THF/H₂O, 55 °C, overnight, 61%; *iii* CuCN, dry NMP, 190 °C, 3 d, 45% for **4**, 48% for **5**.

Donor substituents (red) at one pyrene side were introduced by reductive alkylation with sodium dithionite and subsequent addition of an alkylation reagent (Scheme 1). In the case of **2**, dimethyl sulfate gave the methylated species.⁹ Treatment of **1** with 2-nitropropane yielded the acetonide **3** in 61%. The ketal structure is a stronger donor and thus holds promise for a decreased energy gap and an increased dipole moment of the respective D–A pyrene derivative.

In order to exchange bromine atoms with a stronger acceptor group (blue) Rosenmund-von Braun conditions using copper(I)cyanide in dry *N*-methylpyrrolidone (NMP) at elevated temperature were applied. Compounds **4** and **5** were obtained in similar yields as orange and red solids, respectively. The color already indicates a narrowed energy gap of the new D–A pyrenes.

The pure donors **7** and **8**¹⁰ could be obtained from pyrene-4,5,9,10-tetraone **6**¹¹ similar to conversion of **1** to

Scheme 2. Synthesis of Donor and Acceptor Pyrenes **7**, **8** and **9**^a



^a Conditions: *i* 2-nitropropane, Na₂CO₃, acetonitrile/THF/H₂O, 55 °C, overnight, 44%; *ii* Na₂S₂O₄, Me₂SO₄, KOH, Bu₄NBr, H₂O/THF, 40 °C, overnight, 62%.

3 and **2**, respectively (Scheme 2). Acceptor **9**¹² is already known but no crystal structure had yet to be reported. Suitable crystals of **3**, **4**, **5**, **7**, **8** and **9** could be grown by standard crystallization procedures, and the structures were confirmed by X-ray crystallography (see Supporting Information).

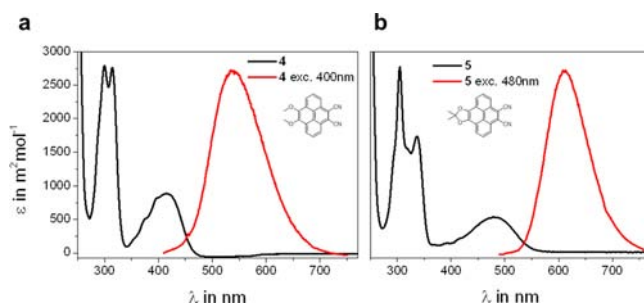


Figure 1. UV–vis absorption (black) and normalized emission (red) spectra of D–A pyrenes (a) **4** and (b) **5** in THF at 10^{−5} M concentration.

Having pure donors **7** and **8**, acceptor **9** as well as D–A pyrenes **4** and **5** in hand, UV–vis absorption and emission properties were investigated in tetrahydrofuran (THF) solutions to quantify the decrease of the energy gap. The spectra of D–A pyrenes are depicted in Figure 1 and the values are listed in Table 1.

Large optical energy gaps ($E_{g(opt)}$) of 2.96, 3.25 and 2.95 eV were found for **7**, **8** and **9** (for spectra see Supporting Information), respectively. The spectra exhibit the vibrational structure of the absorption bands. The absorption and emission spectra of D–A pyrenes **4** and **5** are of similar shape (Figure 1). The absorption maximum

(9) Zöphel, L.; Beckmann, D.; Enkelmann, V.; Chercka, D.; Rieger, R.; Müllen, K. *Chem. Commun.* **2011**, 47, 6960–6962.

(10) 4,5,9,10-Tetramethoxypyrene **8** has already been described but without experimental procedure, see: Medjanik, K.; Chercka, D.; Nagel, P.; Merz, M.; Schuppler, S.; Baumgarten, M.; Müllen, K.; Nepijko, S. A.; Elmers, H. J.; Schonhense, G.; Jeschke, H. O.; Valenti, R. *J. Am. Chem. Soc.* **2012**, 134, 4694–4699.

(11) Hu, J.; Zhang, D.; Harris, F. W. *J. Org. Chem.* **2005**, 70, 707–708.

(12) Shimizu, S.; Nakano, S.; Hosoya, T.; Kobayashi, N. *Chem. Commun.* **2011**, 47, 316–318.

at the longest wavelength of the acetone **5** is red-shifted by 65 nm compared to **4** which corresponds to a decrease of the $E_{\text{g(opt)}}$ by 0.43 eV. Fixing the oxygen atoms in a five-membered ring enhances electron-donating character of the oxygen lone-pairs, and thus, raises the HOMO level to a larger extent. Quantum mechanical calculations using Gaussian (DFT/B3LYP/6-31G(d)) in vacuum confirmed the decrease of the energy gap. In contrast to **7**, **8** and **9**, the absorption band of the longest wavelength appears broadened for the D–A pyrenes. In related work on 2,7-D-A substituted 4,5,9,10-tetrahydropyrenes, a similarly broad long wavelength band was described which could be assigned to arise from intramolecular charge-transfer (ICT).^{4b,c} Furthermore, a strong increase of the dipole moment from the ground state to the excited state was reported together with a pronounced dependency of the emission wavelength on the solvent polarity.

Table 1. Optical Properties of Compounds **4**, **5**, **7**, **8** and **9**^a

	λ_{abs}^b [nm]	λ_{em}^c (λ_{ex}^d) [nm]	λ_{edge} [nm]	$E_{\text{g(opt)}}^e$ [eV]	$E_{\text{g(cal)}}^f$ [eV]	μ^d [D]
4	415	536 (400)	461	2.69	3.18	8.8
5	480	613 (480)	549	2.26	2.72	9.2
7	411	418 (380)	419	2.96	3.32	0.0
8	388	385 (350)	382	3.25	3.73	0.0
9	412	418 (291)	421	2.95	3.34	0.1

^a All absorption and emission spectra were measured in THF. ^b λ_{abs} is the absorption band appearing at the longest wavelength. ^c λ_{em} is the fluorescence band appearing at the shortest wavelength. ^d λ_{ex} wavelength of excitation. ^e Calculated from λ_{edge} . ^f Calculated by DFT/B3LYP/6-31G(d) using Gaussian.

Such solvatochromism was also expected for D–A pyrenes **4** and **5**. Strong bathochromic shifts of the emission could be observed by increasing polarity from cyclohexane to THF by 62 and 92 nm for **4** and **5**, respectively (Figure S12, Supporting Information). This pronounced effect is explained by better stabilization of the excited state with increasing solvent polarity.¹³ It can be concluded from the larger red-shift that **5** undergoes a larger change of the molecular dipole moment (μ) upon excitation than **4**. As expected, negligible solvatochromism of the emission was observed for compounds **7**, **8** and **9**. These findings are supported by calculations of the dipole moment in the ground state of structures **4**, **5**, **7**, **8** and **9** (Table 1). Whereas no dipole is predicted for pure donors **7**, **8** and acceptor **9**, the D–A substitution induces dipoles of 8.8 and 9.2 D, respectively, for **4** and **5**.

In order to determine the impact of the different K-region substitution on the frontier orbitals, cyclic voltammetry (CV) was performed. The cyclic voltammograms are shown in Figure S13 (see Supporting Information), and the extracted values are listed in Table 2. Under measurement conditions for donors **7** and **8**, a reversible oxidation

Table 2. Electronic Properties of Compounds **4**, **5**, **7**, **8** and **9** Experimentally (CV) and Calculated

	E_{HOMO}^a [eV]	E_{LUMO}^a [eV]	$E_{\text{g(CV)}}^b$ [eV]	E_{HOMO}^c [eV]	E_{LUMO}^c [eV]
4	−5.82	−3.22	2.60	−5.90	−2.72
5	−5.50	−3.26	2.24	−5.44	−2.72
7	−5.13	^d	^d	−4.63	−1.31
8	−5.43	^d	^d	−5.06	−1.33
9	^d	−3.52	^d	−6.69	−3.35

^a Determined by cyclic voltammetric measurement in 0.1 M *n*-Bu₄NPF₆/CH₂Cl₂ with scan rates between 50 mV/s and 100 mV/s; values calculated using the ferrocene HOMO level: $E_{\text{HOMO(CV)}} = -(E_{\text{ox,onset}} - E^{(1/2)}_{\text{Fc/Fc}^+} + 4.8)$ eV. ^b Calculated from CV E_{HOMO} and E_{LUMO} . ^c Calculated by DFT/B3LYP/6-31G(d) using Gaussian. ^d Could not be determined under measurement conditions.

wave could be observed which corresponds to the highest occupied molecular orbital (HOMO) at −5.13 eV (**7**) and −5.43 eV (**8**). For acceptor **9** an irreversible reduction wave was found giving a value of −3.52 eV for the lowest unoccupied molecular orbital (LUMO).

In case of the D–A substituted pyrenes **4** and **5**, both processes (oxidation and reduction) could be measured due to a narrowed energy gap. **4** exhibits a reversible reduction and irreversible oxidation process giving an energy gap ($E_{\text{g(CV)}}$) of 2.60 eV. Oxidation and reduction of **5** proceeds reversibly and $E_{\text{g(CV)}}$ was determined as 2.24 eV. The energy gaps obtained from CV measurements are almost identical to the optical energy gaps of 2.69 and 2.26 eV, respectively. CV further revealed that the LUMO levels of **4** and **5** are nearly identical (same acceptor moiety) but the HOMO level of **5** is raised by 0.32 eV because of the stronger donor moiety.

Calculated orbital surfaces of **4** and **5** visually support the influence of the D–A substitution (Figure S14, Supporting Information). The biggest orbital coefficients were found at the donor side in the HOMO and at the acceptor side in the LUMO. It is important to note that the usual nodal plane in the 2–7 direction of the substituted pyrenes is lost for the asymmetric 4,5 and 9,10 substitution. This supports the assumption of an intramolecular charge transfer taking place between the donor and acceptor side.

Beside the structural proof, X-ray crystallography was used to investigate the impact of the D–A substitution on the solid state order. The crystal packing is depicted in Figure 2. For all five molecules, the pyrene core was found to be planar. The *ortho*-methoxy groups of **4** and **8** are twisted out of the pyrene plane oppositely. The packing of **9** is strongly influenced by the bulky *tert*-butyl groups, and thus, no π – π stacking was observed. A similar arrangement was found for **8** without any parallel overlap of the pyrene planes being best described as a herringbone motif without π – π interactions due to an offset of the molecules.

The packing of D–A pyrenes **4** and **5** is featured by stacks of the molecules with an alternating rotation by 180°. In this way the donor side is located on top of the acceptor side and vice versa. Distances of 3.38 Å (**4**) and

(13) (a) Valeur, B. *Molecular Fluorescence: Principles and Applications*; Wiley-VCH: Verlag GmbH, 2001. (b) Reichardt, C. *Chem. Rev.* **1994**, *94*, 2319–2358.

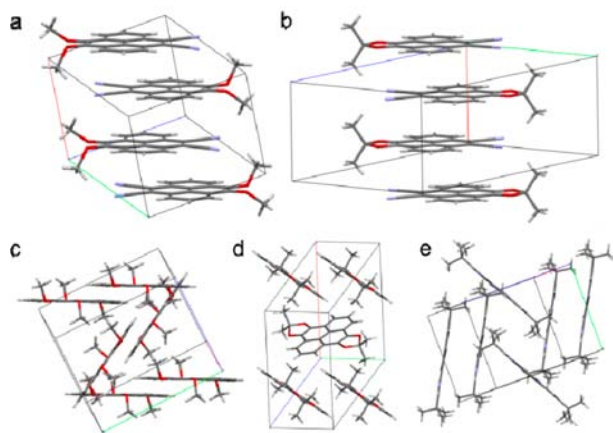


Figure 2. Crystal packing of D–A pyrenes (a) **4**, (b) **5**, donors (d) **7**, (c) **8** and acceptor (e) **9**.

3.41 Å (**5**) were determined for the π – π stacking between the planar molecules. Although crystallization is a complex process and is determined by a large number of parameters, it is generally believed that the tendency for antiparallel molecular arrangements increases with the dipolar characteristics of a molecule.¹⁴ Accordingly, it seems that besides other factors like the spatial influence of the bulky methoxy groups and π – π -interactions, the D–A substitution has an impact on the orientation of the molecules via intermolecular electrostatic forces. Furthermore, **4** and **5** were found to crystallize in centrosymmetric space groups. A detailed study by Desiraju et al. showed a strong

tendency towards centrosymmetry for conjugated or aromatic molecules with large dipole moments.¹⁴

In conclusion, the synthesis of two double D–A substituted pyrenes in the K-region based on asymmetrically functionalized 9,10-dibromopyrene-4,5-dione was presented. In comparison to the pure donor and acceptor pyrenes, the UV–vis absorption of D–A pyrenes proved a significant decrease of the optical energy gap as a consequence of an intramolecular charge transfer. Accordingly, a raised HOMO level and a smaller energy gap could be implemented by the choice of a stronger donor moiety. Furthermore, pronounced solvatochromism was observed for both D–A pyrenes which makes these molecules potential candidates as solvent polarity sensors. X-ray analysis revealed an antiparallel packing induced by the dipoles of the push–pull molecules. These findings underline the potential and effectiveness of this approach to engineer pyrene's optoelectronic properties and solid state packing. Current efforts are focused on the introduction of stronger electron-withdrawing and -donating groups to strengthen the intramolecular charge-transfer and the thereof resulting properties.

Acknowledgment. We thank the German Federal Ministry of Education and Research (BMBF) and Evonik Industries for financial support within the MaDriX project.

Supporting Information Available. Full experimental procedures and characterization data. CIF files from the X-ray analysis of **3**, **4**, **5**, **7**, **8** and **9**—CCDC 874828, 874821, 874825, 907946, 910642 and 874822. This material is available free of charge via the Internet at <http://pubs.acs.org>.

(14) Dey, A.; Desiraju, G. R. *Chem. Commun.* **2005**, 2486–2488.

The authors declare no competing financial interest.